For example, 'Stage 1' of the original scoring system was defined as 'sparse Lewy bodies or neurites.' On the other hand, 'Grade 1'of our methodology is defined as 'sparse Lewy neurites without Lewy bodies.'

Grade 0 = neither LNs nor LBs detected using anti-phosphorylated α-synuclein antibody.

Grade 1 = sparse phosphorylated α-synuclein immunopositive dots or neurites, or diffuse granular cytoplasmic stain in the neuron, neither LBs nor phosphorylated α-synuclein-immunopositive neuronal intracytoplasmic dense aggregations.

Grade 2 = 1–3 LBs or phosphorylated α-synuclein-immunopositive intracytoplasmic dense aggregations and scattered LNs in a low-power field (×10).

Grade 3 = more than four LBs and scattered LNs in a low-power field (×10).

Grade 4 = numerous LBs and neurites with severe immunoreactivity for phosphorylated α-synuclein in the neuropil or background.

LB staging system of our BBAR (BBAR LB stage)

In order to assess the clinical and neuropathologic alterations of LBD, we applied the following rating system to our BBAR for all autopsy cases (Table 2, Fig. 3). The original BBAR LB staging system was developed in order to track the individual data of our brain bank.[24,25] This rating system requires clinical symptoms, gross and microscopic neuropathologic alterations, and LB scores used in the consensus guidelines for the clinical and pathologic diagnosis of DLB.[27] In this staging system, Parkinson's disease with

Table 2 Lewey body stage of Brain Bank for Aging Research

Stage	Psyn-IR	LB	SN: loss of pigmentation	LB score	Dementia	Parkinsonism	Diagnosis
0	–	–	–				
0.5	+	–	–				
1	+	+	–				Incidental LBD
2	+	+	+	0–10	–†	–†	Subclinical LBD
3	+	+	+	0–10	–	+	PD
4	+	+	+	3–6	+	+	PDDL
	+	+	+	3–6	+	+ or –	DLBL‡
5	+	+	+	7–10	+	+	PDDN
	+	+	+	7–10	+	+ or –	DLBN‡

†Neither dementia nor Parkinsonism associated with Lewy body-related α-synucleinopathy. ‡Differential diagnosis of PDD and DLB was based on the '1-year rule' according to the consensus guidelines (34). DLBL, dementia with Lewy bodies and a Lewy body score corresponding to the limbic form; DLBN, dementia with Lewy bodies and a Lewy body score corresponding to the neocortical form; LB, Lewy body; LBD, Lewy body disease; PD, Parkinson's disease; PDDL, Parkinson's disease with dementia and a Lewy body score corresponding to the limbic form; PDDN, Parkinson's disease with dementia and a Lewy body score corresponding to the neocortical form; Psyn-IR, phosphorylated alpha-synuclein immunoreactivity; SN, substantia nigra.

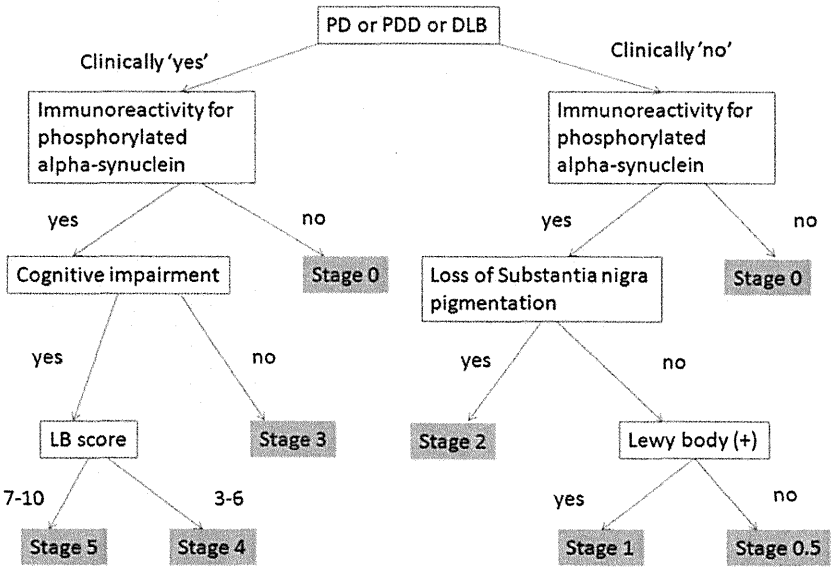

Fig. 3 Flow-chart of the Lewy body staging system of the Brain Bank for Aging Research (BBAR). PD, Parkinson's disease; PDD, Parkinson's disease with dementia; DLB, dementia with Lewy bodies; SN, substantia nigra; LB score, Lewy body score. See Table 2 for detailed description of each stage.

dementia was differentiated from DLB by applying the '12-month (1-year)' rule noted in the Consensus Guidelines (i.e., 'dementia appears more than one year after the onset of Parkinsonism').[27]

Evaluation of senile changes and neuropathologic diagnosis

NFTs were classified according to Braak and Braak's staging system using modified Gallyas-Braak staining[37] and AT8 immunohistochemistry.[38] The staging system for senile plaques (SPs) comprises four stages (0–C). Argyrophilic grains were classified into our four stages (0–III), as reported previously.[23] The neuropathologic diagnosis of Alzheimer disease was based on our previous definition,[39] which proposed a modification of the National Institute on Aging and Reagan Institute criteria.[40,41] The diagnoses of dementia with grains and NFT-predominant forms of dementia were based on the previously described definitions.[42,43]

Statistical analysis

Fisher's exact test was carried out to compare the number of cases having LBAS pathology in the olfactory mucosa.

RESULTS

Clinical information

Of the 105 consecutive autopsy patients, 58 were men and 47 were women. The patient ages at death ranged from 65 to 104 years (82 ± 37, mean ± SD). Twelve patients showed Parkinson's disease-related symptoms according to the clinical criteria in this study. Six out of 105 patients were clinically diagnosed as LBD including Parkinson's disease, Parkinson's disease with dementia and DLB.

Neuropathologic diagnosis

The neuropathologic diagnoses consisted of Alzheimer disease ($n = 15$), dementia with grains ($n = 11$), NFT-predominant form of dementia ($n = 8$), Parkinson's disease ($n = 2$), Parkinson's disease with dementia ($n = 2$), and DLB ($n = 1$), as well as one case each of dentatorubral-pallidoluysian atrophy, neuronal hyaline inclusion body disease, frontotemporal lobar degeneration with transaction response (TAR) DNA-binding protein-43 kDa-immunoreactive inclusions, and progressive multifocal leukoencephalopathy. Patients with combined pathologies, included Alzheimer's disease plus DLB ($n = 2$), dementia with grains plus NFT-predominant form of dementia ($n = 3$), and one patient each of diffuse NFTs with calcification (DNTC)[44] plus DLB and dementia with grains plus Alzheimer's disease. The remaining patients did not fulfil the clinical and/or pathological criteria for neurodegenerative diseases.

Eight out of 105 patients (8/105 = 7.6%) were clinically and neuropathologically diagnosed as having LBD, including Parkinson's disease (2 patients), Parkinson's disease with dementia (2 patients) and DLB (4 patients).

Incidence, distribution and extent of LBAS

BBAR staging

Based on clinical and neuropathologic analyses, the BBAR LB stages were as follows: stage 0 = 66 cases, stage 0.5 = 6 cases, stage 1 = 21 cases, stage 2 = 4 cases, stage 3 = 2 cases, stage 4 = 3 cases and stage 5 = 3 cases. All of the stage 5 cases had DLB, with an LB score corresponding to the value for the neocortical form (DLBN).

LBAS in CNS and peripheral nervous system

We identified 39 (37.1%) out of the 105 individuals with α-synuclein immunopositive LBAS in the CNS or peripheral nervous system (Table 3). Therefore, we focused on these 39 cases in the present study. Here, LBAS was identified by using α-synuclein immunohistochemistry. In LBAS, LBs were confirmed with HE stains and α-synuclein immunohistochemistry. Out of the 39 cases, 33 showed LBAS in the olfactory bulb, 15 in the enteric nerve plexus, 23 in the sympathetic ganglia, and 16 in the pericardial nerve fibers of the left ventricle (Tables 3 and 4).

Olfactory mucosa

The olfactory epithelium is a pseudostratified columnar epithelium lying deep within the recess of the superior nasal cavity; it is composed of a mixture of multipotential stem cells (basal cells), supporting cells and olfactory receptor neurons (Fig. 2). Mature neurons are reported to give rise to fine and unmyelinated axons that ascend through the cribriform plate to synapse at glomeruli in the olfactory bulb.[20,45]

LBAS were found in the olfactory mucosa of seven (17.9%) out of 39 cases (Tables 3 and 4). These seven also had LBAS in the olfactory bulb. LBAS was present in the lamina propria mucosa of the seven cases (Fig. 4a–c). In addition, one case showed LBAS in a bundle of axons in the cribriform plate (Fig. 4d). None of the cases showed LBAS in the olfactory epithelial paraneuron. We summarized the demographic results of these seven individuals with LBAS in the olfactory mucosa in Table 5. Neither phosphorylated tau-positive deposits nor amyloid β immunopositive deposits were detected in the olfactory mucosa.

Table 3 The distribution of α-synuclein deposits in various anatomical regions of 39 cases with Lewy body disease

Age at death/gender	Parietal lobe	Frontal lobe	Temporal lobe	Cingulate gyrus	Entorhinal cortex	Amygdala	Olfactory bulb	Nucleus basalis of Meynert	Substantia nigra	Locus coeruleus	Dorsal motor nucleus of the vagus	Spinal Cord	Gastrointestinal system	Olfactory Mucosa	Sympathetic ganglion	Adrenal gland	Pericardial nerve	Skin	BBAR LB stage	NFT stage	SP stage
104/F																			5	4	C
70/F																			5	4	C
86/F																			5	6	C
84/M																			4	2	A
79/F																			4	2	A
80/F																			4	2	A
81/M																			3	2	A
88/M																			3	3	A
79/M																			2	1	A
68/F																			2	2	B
79/F																			2	6	C
77/F																			2	6	C
78/M																			1	2	A
75/M																			1	2	A
89/F																			1	3	C
93/F																			1	4	C
86/M																			1	4	C
81/M																			1	2	A
90/F																			1	2	A
86/M																			1	2	A
97/F																			1	2	A
78/M																			1	1	A
92/M																			1	3	C
94/M																			1	4	A
85/M																			1	3	A
81/F																			1	5	C
96/F																			1	2	0
87/F																			1	3	A
101/F																			1	4	A
69/F																			1	4	0
83/F																			1	3	A
72/M																			1	1	A
77/M																			1	2	A
83/M																			0.5	4	C
71/M																			0.5	2	A
89/M																			0.5	2	A
85/F																			0.5	3	A
85/F																			0.5	2	A
96/F																			0.5	3	A

Grade 0 = blank, grade 1 = light grey, grade 2 = light blue, grade 3 = blue, grade4 = navy blue. The number in each cell indicates a score based on the semiquantitative scoring system of Lewy-related pathology. 0 = neither Lewy neurites nor bodies detected by using anti-phosphorylated α-synuclein antibody. 1 = sparse phosphorylated α-synuclein immunopositive dots or neurites, neither Lewy bodies nor phosphorylated α-synuclein immunopositive intracytoplasmic aggregations. 2 = one to three Lewy bodies or phosphorylated α-synuclein immunopositive intracytoplasmic aggregations in a low-power field (×10). 3 = more than four Lewy bodies and scattered Lewy neurites in a low-power field (×10). 4 = numerous LBs and neurites with severe immunoreactivity for phosphorylated α-synuclein in the neuropil or background. Individuals of BBAR LB stages 3–5, with clinical Parkinsonism and neuropathologically numerous LBASs in the CNS, showed high incidence (75%, 6/8 individuals) of LBASs in the olfactory mucosa. In contrast, individuals of BBAR LB stages 1–3 without Parkinsonism showed extremely low incidence of Lewy body-related α-synucleinopathy (LBAS) (3%, 1/31) in the olfactory mucosa. LBAS was found in the olfactory mucosa mostly in advanced BBAR LB stages 3–5. BBAR LB Brain Bank for Aging Research Lewy body staging, NFT stage, Braak's stages for neurofibrillary tangles; SP stage, Braak's stages for senile plaques.

Table 4 Regional frequency of Lewy body-related α-synucleinopathy (LBAS) in various anatomical regions

The BBAR LB stage	Olfactory epithelium	Olfactory mucosa	Olfactory bulb	Spinal cord	GI tract	Sympathetic ganglia	Adrenal gland	Pericardial nerve	Skin
0.5	0/6	0/6	2/6	0/6	0/6	2/6	0/6	1/6	0/6
1	0/21	1/21	19/21	7/21	6/27	10/21	1/21	6/21	1/21
2	0/4	0/4	4/4	3/4	1/4	3/4	0/4	2/4	0/4
3	0/2	1/2	2/2	2/2	2/2	2/2	2/2	1/2	2/2
4	0/3	3/3	3/3	3/3	3/3	3/3	3/3	3/3	2/3
5	0/3	2/3	3/3	3/3	3/3	3/3	1/3	3/3	0/3
All	**0/39**	**7/39**	**33/39**	**18/39**	**15/39**	**23/39**	**7/39**	**16/39**	**5/39**

BBAR LB Brain Bank for Aging Research Lewy body staging.

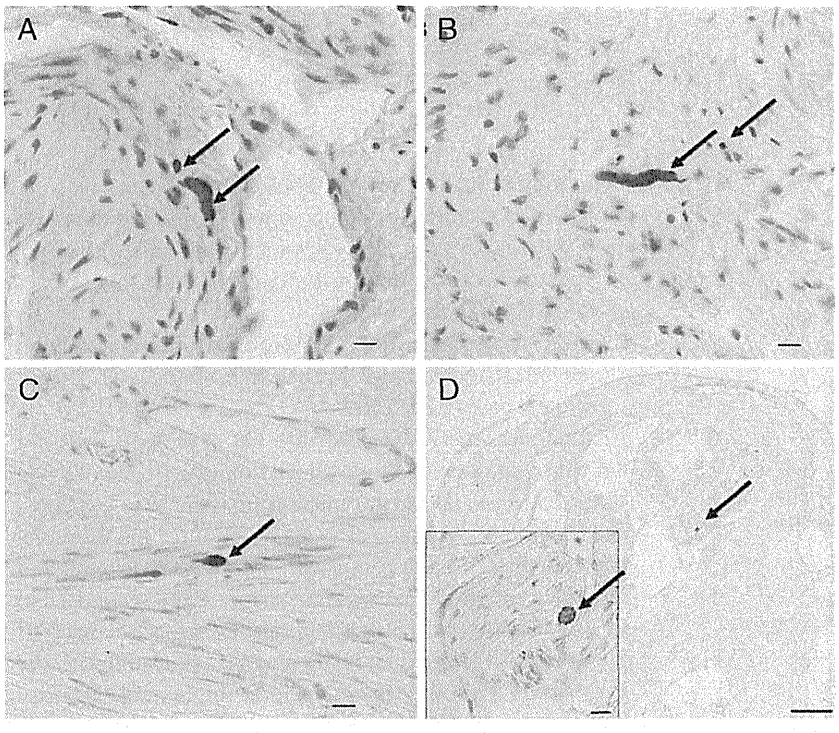

Fig. 4 Photomicrographs show α-synuclein immunopositive deposits (arrows indicate Lewy neurites) in the axonal bundle of the lamina propria (a–c) and cribriform plate (d). The inset in figure (d) shows a higher magnification image of α-synuclein immunopositive deposits in the axonal bundle of the cribriform plate. Immunohistochemistry using monoclonal antibody against phosphorylated α-synuclein (pSyn#64). Photomicrographs (a, b, c and d) were obtained from cases 4, 5, 7 and 3, respectively, in Table 5. (a–c), scale bar = 10 μm; (d) scale bar = 100 μm (inset, 10 μm).

Correlations between α-synuclein immunopositive LBs or LNs in the olfactory mucosa and CNS

Alpha-synuclein immunopositive LBs or LNs in the olfactory mucosa were detected in seven cases, including three with DLB, three with Parkinson's disease or Parkinson's disease with dementia, and one with incidental LBD (Tables 3–5). LBAS in the olfactory mucosa was compared with those in other locations of the CNS (Table 3). Individuals of BBAR LB stages 3–5, clinical and neuropathological diagnosis of LBD, showed a high incidence (75%, 6/8 individuals) of α-synuclein immunopositive LBAS in the olfactory mucosa (Table 6, Fig. 5). Six individuals with Parkinson's disease also showed a high incidence of α-synuclein accumulation (66%, 4/6 individuals) in the olfactory mucosa. In contrast, individuals of BBAR LB stages 0.5–2 (here we classified them into asymptomatic group) showed a low incidence of LBAS (3%, 1/31) in the olfactory mucosa.

Olfactory bulb

There is neural connectivity among olfactory receptor neurons and nuclei in the olfactory bulbs.[45] Hence, we analyzed the frequency of LBAS in the glomeruli, tufted cells, mitral cells and granular cells between LBAS-positive and LBAS-negative groups in the olfactory epithelium.

In individuals of BBAR LB stages 3–5 (symptomatic stage), LBAS was frequently observed in the glomeruli (8/8 cases, 100%), granular cells (8/8, 100%) and tufted cells (7/8, 87.5%). In contrast, there were low numbers of cases with LBAS in the mitral cells (2/8, 25%). Asymptomatic stage cases of LBD, corresponding to BBAR stage 0.5–2,

Table 5 Clinical and neuropathological demography of seven individuals with Lewy body-related α-synucleinopathy (LBAS) identified in the olfactory mucosa

No.	Age at death	Clinically diagnosed as LBD	Cause of death	Neuropathologic diagnosis	BBAR LB stage	LBAS in the olfactory mucosa			NFT stage	SP stage
						Olfactory epithelium	Lamina propria mucosa	Cribriform plate		
1	104/F	None	CHF, MI, Dementia	DLBN, AD	5	0	1	0	1	C
2	70/F	DLB	DLB, pneumonia	DLBN, AD	5	0	1	0	1	C
3	84/M	DLB	Prostate carcinoma, DLB	DLBL	4	0	1	1	2	A
4	79/F	PDD	PDD	PDDN	4	0	1	0	2	A
5	80/F	PD	Pneumonia, PD	PDDL	4	0	1	0	2	A
6	88/M	PD	Pneumonia, PD	PD	3	0	1	0	2	A
7	86/M	None	Pneumonia	AD,Incidental LBD	1	0	1	0	1	C

AD, Alzheimer's disease; BBAR LB stage, Lewy body staging system of the Brain Bank for Aging Research; CHF, congestive heart failure; DLB, dementia with Lewy bodies; DLBL, dementia with Lewy bodies and a Lewy body score corresponding to the limbic form; DLBN, dementia with Lewy bodies and a Lewy body score corresponding to the neocortical form; F, female; LB, Lewy body; LBD, Lewy body disease; M, male; MI, acute myocardial infarction; NFT stage, Braak's stages for neurofibrillary tangles; PD, Parkinson's disease; PDDL, Parkinson's disease with dementia and a Lewy body score corresponding to the limbic form; PDDN, Parkinson's disease with dementia and a Lewy body score corresponding to the neocortical form; SP stage, Braak's stages for senile plaques.

Table 6 Incidence of LBAS in the olfactory mucosa in cases with symptomatic LBD (BBAR stage 3–5)

Clinical and neuropathologic diagnosis of LBD	LBAS in OM		Total
	Present	Absent	
Symptomatic (BBAR 3–5)	6*	2	8
Asymptomatic (BBAR 0.5–2)	1	30	31

*$P < 0.05$. BBAR, Brain Bank for Aging Research; LBAS; Lewy body-related alpha-synucleinopathy; LBD, Lewey body disease; OM; olfactory mucosa.

showed high incidence of LBAS in the glomeruli (23/31, 74.1%) and granular cells (22/31, 70.9%) of the olfactory bulb (Fig. 5).

DISCUSSION

Our study provides two novel observations.

1 LBAS in the olfactory mucosa was frequently observed (6/8 cases, 75%) in the symptomatic patients with LBD, but was a rare condition (1/31 cases, 3.2%) in asymptomatic LBD patients.

2 LBAS was seen in the glomeruli and granular cells in the olfactory bulbs of most symptomatic and asymptomatic cases with LBD.

It has been widely accepted that LB pathology does not develop simultaneously in all anatomical regions of the central and peripheral nervous systems. Hawkes *et al.* proposed that neurotropic pathogens may enter the brain via two routes: (i) a nasal route, with anterograde progression into the temporal lobe; and (ii) a gastric route secondary to the swallowing of nasal secretions in saliva (a dual hit hypothesis).[46] The former route may be associated with the early accumulation of α-synuclein in the human olfactory bulb and cause olfactory dysfunction in sporadic Parkinson's disease. In the present study, there was rare observation of LBAS in the olfactory mucosa in the asymptomatic cases of LBD. Further analysis is important to clarify the possibility of propagation of α-synuclein in the nervous systems.

In the present study, LBAS was frequently observed in the olfactory mucosa (6/8 cases, 75%) in the individuals with clinical LBD. In contrast, LBAS in the olfactory mucosa was a rare observation in asymptomatic patients. It is also important that all seven cases with LBAS in the olfactory mucosa had LBAS in the cerebral cortex and brainstem. Our results have similarities with a previous report concerning Alzheimer's disease.[20] Detection of LBAS in the olfactory mucosa could be hindered by two problems: technical difficulty in obtaining enough nerve fibers and rapid turnover of olfactory receptor neurons.[47,48] In fact, a recent study reported that a biopsy study revealed no α-synuclein immunopositive deposits in the olfactory

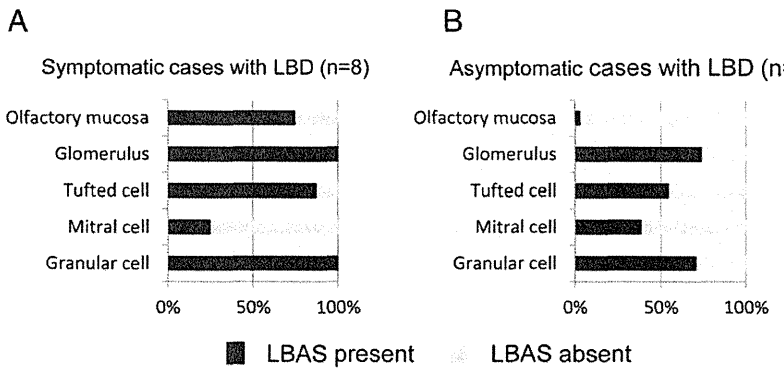

Fig. 5 Frequencies of cases having Lewy-related α-synucleinopathy (LBAS) pathology in the olfactory mucosa and each anatomical region of the olfactory bulb. (a) Cases with symptomatic dementia with Lewy bodies (LBD) ($n = 8$, Brain Bank for Aging Research [BBAR] stages 3–5). Most of the cases show LBAS pathology in the olfactory mucosa (6/8, 75%), glomeruli (8/8, 100%), tufted cells (6/7, 85.7%) and granular cells (8/8, 100%). The number of cases with LBAS in the mitral cells is low (2/6, 33.3%). (b) Cases with asymptomatic LBD ($n = 25$, BBAR stages 0.5–2). Most of the cases show LBAS pathology in the glomeruli (23/31, 74.1%), tufted cells (17/31, 54.8%) and granular cells (22/31, 70.9%). The number of cases with LBAS in the mitral cells (12/31, 38.7%) is low. LBAS pathology of the olfactory mucosa is present in only one case (1/31, 3.2%).

mucosa of patients of Parkinson's disease.[21] Our previous study indicated a high incidence of α-synuclein immunopositive LBs or neurites in aging human olfactory bulbs, and suggested that they extend from the periphery (the second olfactory structure) to the anterior olfactory nucleus (the tertiary olfactory structure).[11] The present study, using 6 μm-thick paraffin embedded sections, revealed that LBAS was most frequently observed in the glomeruli which were composed of axon terminals of olfactory epithelial cells and dendrites of mitral and tufted cells[45] as well as in the glomerular cells which were most numerous in the periphery of the olfactory bulb (Fig. 5). We consider that high incidence of LBAS in glomeruli may represent affected terminal axons of olfactory epithelial neurons. In contrast to our result, a previous study, employing 50 μm-thick floating sections, reported high frequency of LBAS in mitral cells and the internal plexiform layer in individuals with Parkinson's disease but no LBAS in age-matched controls.[49] Further studies are necessary to identify the most vulnerable subset in the periphery of the olfactory bulb.

In conclusion, presence of LBAS in the olfactory mucosa and olfactory glomeruli further supports the importance of olfactory system as an entry zone of LBD. Future studies of LB pathology involving the olfactory system are indicated to understand the pathomechanism of α-synuclein accumulation in individuals with LBD.

ACKNOWLEDGMENTS

This study was supported in part by a Grant-in-Aid for Scientific Research (Kakenhi B) (20390248) (SM), The Specified Disease Treatment Research Program (SM), Research on Measures for Intractable Diseases (MT) (H23-nanchi-ippan-062, H24-nanchi-ippan-063, Nanchi-ippan-013), and the Comprehensive Brain Science Network (SM, MT). We gratefully acknowledge Naoo Aikyo, Fumio Hasegawa, Mieko Harada, Yuki Kimura, Nobuko Naoi and Sachiko Imai for technical help. We thank Dr. T. Iwatsubo (Department of Neuropathology, University of Tokyo, Tokyo, Japan) for the kind gifts of antibodies and Dr. K. Suzuki (Department of Neuropathology, Tokyo Metropolitan Geriatric Hospital and Institute of Gerontology) for useful discussions and comments.

Portions of this study were presented at the 86th annual meeting of the American Association of Neuropathologists, Philadelphia, in 2010.

REFERENCES

1. Baba M, Nakajo S, Tu PH *et al.* Aggregation of alpha-synuclein in Lewy bodies of sporadic Parkinson's disease and dementia with Lewy bodies. *Am J Pathol* 1998; **152**: 879–884.
2. Spillantini MG, Crowther RA, Jakes R, Hasegawa M, Goedert M. alpha-Synuclein in filamentous inclusions of Lewy bodies from Parkinson's disease and dementia with Lewy bodies. *Proc Natl Acad Sci U S A* 1998; **95**: 6469–6473.
3. Goedert M, Spillantini MG, Davies SW. Filamentous nerve cell inclusions in neurodegenerative diseases. *Curr Opin Neurobiol* 1998; **8**: 619–632.
4. Ogunnyi A, Akang EE, Gureje O *et al.* Dementia with Lewy bodies in a Nigerian: a case report. *Int Psychogeriatr* 2002; **14**: 211–218.
5. Takao M, Ghetti B, Yoshida H *et al.* Early-onset dementia with Lewy bodies. *Brain Pathol* 2004; **14**: 137–147.
6. Braak H, Ghebremedhin E, Rub U, Bratzke H, Del Tredici K. Stages in the development of Parkinson's disease-related pathology. *Cell Tissue Res* 2004; **318**: 121–134.
7. Braak H, Sastre M, Bohl JR, de Vos RA, Del Tredici K. Parkinson's disease: lesions in dorsal horn layer I,

involvement of parasympathetic and sympathetic pre- and postganglionic neurons. *Acta Neuropathol* 2007; **113**: 421–429.
8. Braak H, Braak E. Pathoanatomy of Parkinson's disease. *J Neurol* 2000; **247** (Suppl 2): II3–I10.
9. Braak H, Del Tredici K, Rub U, de Vos RA, Jansen Steur EN, Braak E. Staging of brain pathology related to sporadic Parkinson's disease. *Neurobiol Aging* 2003; **24**: 197–211.
10. Del Tredici K, Rub U, De Vos RA, Bohl JR, Braak H. Where does Parkinson disease pathology begin in the brain? *J Neuropathol Exp Neurol* 2002; **61**: 413–426.
11. Sengoku R, Saito Y, Ikemura M *et al.* Incidence and extent of Lewy body-related alpha-synucleinopathy in aging human olfactory bulb. *J Neuropathol Exp Neurol* 2008; **67**: 1072–1083.
12. Ponsen MM, Stoffers D, Booij J, van Eck-Smit BL, Wolters ECh, Berendse HW. Idiopathic hyposmia as a preclinical sign of Parkinson's disease. *Ann Neurol* 2004; **56**: 173–181.
13. Haehner A, Boesveldt S, Berendse HW *et al.* Prevalence of smell loss in Parkinson's disease – a multicenter study. *Parkinsonism Relat Disord* 2009; **15**: 490–494.
14. Daniel SE, Hawkes CH. Preliminary diagnosis of Parkinson's disease by olfactory bulb pathology. *Lancet* 1992; **340** (8812): 186.
15. Pearce RK, Hawkes CH, Daniel SE. The anterior olfactory nucleus in Parkinson's disease. *Mov Disord* 1995; **10**: 283–287.
16. Beach TG, White CL 3rd, Hladik CL *et al.* Olfactory bulb alpha-synucleinopathy has high specificity and sensitivity for Lewy body disorders. *Acta Neuropathol* 2009; **117**: 169–174.
17. Parkkinen L, Silveira-Moriyama L, Holton JL, Lees AJ, Revesz T. Can olfacotry bulb biopsy be justified for the diagnosis of Parkinson's disease? Comments on 'olfactory bulb α-synucleinopathy has specificity and sensitivity for Lewy body disorders'. *Acta Neuropathol* 2009; **117** (2): 213–214.
18. Jellinger KA. Olfactory bulb α-synucleinopathy has specificity and sensitivity for Lewy body disorders. *Acta Neuropathol* 2009; **117** (2): 215–216.
19. Duda JE, Shah U, Arnold SE, Lee VM, Trojanowski JQ. The expression of alpha-, beta-, and gamma-synucleins in olfactory mucosa from patients with and without neurodegenerative diseases. *Exp Neurol* 1999; **160**: 515–522.
20. Arnold SE, Lee EB, Moberg PJ *et al.* Olfactory epithelium amyloid-beta and paired helical filament-tau pathology in Alzheimer disease. *Ann Neurol* 2010; **67**: 462–469.
21. Witt M, Bormann K, Gudziol V *et al.* Biopsies of olfactory epithelium in patients with Parkinson's disease. *Mov Disord* 2009; **24**: 906–914.
22. Fumimura Y, Ikemura M, Saito Y *et al.* Analysis of the adrenal gland is useful for evaluating pathology of the peripheral autonomic nervous system in Lewy body disease. *J Neuropathol Exp Neurol* 2007; **66**: 354–362.
23. Saito Y, Ruberu NN, Sawabe M *et al.* Staging of argyrophilic grains: an age-associated tauopathy. *J Neuropathol Exp Neurol* 2004; **63**: 911–918.
24. Saito Y, Ruberu NN, Sawabe M *et al.* Lewy body-related alpha-synucleinopathy in aging. *J Neuropathol Exp Neurol* 2004; **63**: 742–749.
25. Saito Y, Kawashima A, Ruberu NN *et al.* Accumulation of phosphorylated alpha-synuclein in aging human brain. *J Neuropathol Exp Neurol* 2003; **62**: 644–654.
26. Ikemura M, Saito Y, Sengoku R *et al.* Lewy body pathology involves cutaneous nerves. *J Neuropathol Exp Neurol* 2008; **67**: 945–953.
27. McKeith IG, Galasko D, Kosaka K *et al.* Consensus guidelines for the clinical and pathologic diagnosis of dementia with Lewy bodies (DLB): report of the consortium on DLB international workshop. *Neurology* 1996; **47**: 1113–1124.
28. Folstein MF, Folstein SE, McHugh PR. 'Mini-mental state'. A practical method for grading the cognitive state of patients for the clinician. *J Psychiatr Res* 1975; **12**: 189–198.
29. Hasegawa K Inoue K, Moriya K. An investigation of dementia rating scale for the elderly. *Seishin Igaku* 1974; **16**: 965–969.
30. Hosokawa T, Yamada Y, Isagoda A, Nakamura R. Psychometric equivalence of the Hasegawa Dementia Scale-Revised with the Mini-Mental State Examination in stroke patients. *Percept Mot Skills* 1994; **79**: 664–666.
31. Lawton MP, Brody EM. Assessment of older people: self-maintaining and instrumental activities of daily living. *Gerontologist* 1969; **9**: 179–186.
32. Morris JC. The Clinical Dementia Rating (CDR): current version and scoring rules. *Neurology* 1993; **43**: 2412–2414.
33. McKhann G, Drachman D, Folstein M, Katzman R, Price D, Stadlan EM. Clinical diagnosis of Alzheimer's disease: report of the NINCDS-ADRDA Work Group under the auspices of Department of Health and Human Services Task Force on Alzheimer's Disease. *Neurology* 1984; **34**: 939–944.
34. McKeith IG, Dickson DW, Lowe J *et al.* Diagnosis and management of dementia with Lewy bodies: third report of the DLB Consortium. *Neurology* 2005; **65**: 1863–1872.

35. Gallyas F. Silver staining of Alzheimer's neurofibrillary changes by means of physical development. *Acta Morphol Acad Sci Hung* 1971; **19**: 1–8.
36. Fujiwara H, Hasegawa M, Dohmae N *et al.* alpha-Synuclein is phosphorylated in synucleinopathy lesions. *Nat Cell Biol* 2002; **4**: 160–164.
37. Braak H, Braak E. Neuropathological stageing of Alzheimer-related changes. *Acta Neuropathol* 1991; **82**: 239–259.
38. Braak H, Alafuzoff I, Arzberger T, Kretzschmar H, Del Tredici K. Staging of Alzheimer disease-associated neurofibrillary pathology using paraffin sections and immunocytochemistry. *Acta Neuropathol* 2006; **112**: 389–404.
39. Murayama S, Saito Y. Neuropathological diagnostic criteria for Alzheimer's disease. *Neuropathology* 2004; **24**: 254–260.
40. Consensus recommendations for the postmortem diagnosis of Alzheimer's disease. The National Institute on Aging, and Reagan Institute Working Group on Diagnostic Criteria for the Neuropathological Assessment of Alzheimer's Disease. *Neurobiol Aging* 1997; **18**: S1–S2.
41. Hyman BT, Trojanowski JQ. Consensus recommendations for the postmortem diagnosis of Alzheimer disease from the National Institute on Aging and the Reagan Institute Working Group on diagnostic criteria for the neuropathological assessment of Alzheimer disease. *J Neuropathol Exp Neurol* 1997; **56**: 1095–1097.
42. Jellinger KA. Dementia with grains (argyrophilic grain disease). *Brain Pathol* 1998; **8**: 377–386.
43. Jellinger KA, Bancher C. Senile dementia with tangles (tangle predominant form of senile dementia). *Brain Pathol* 1998; **8**: 367–376.
44. Kosaka K. Diffuse neurofibrillary tangles with calcification: a new presenile dementia. *J Neurol Neurosurg Psychiatry* 1994; **57**: 594–596.
45. Hawkes CH, Doty RL. *The Neurology of Olfaction.* Cambridge, UK: Cambridge University Press, 2009; 16–21.
46. Hawkes CH, Del Tredici K, Braak H. Parkinson's disease: a dual-hit hypothesis. *Neuropathol Appl Neurobiol* 2007; **33**: 599–614.
47. Graziadei PP, Okano M. Neuronal degeneration and regeneration in the olfactory epithelium of pigeon following transection of the first cranial nerve. *Acta Anat (Basel)* 1979; **104**: 220–236.
48. Graziadei PP, Monti Graziadei AG. Regeneration in the olfactory system of vertebrates. *Am J Otolaryngol* 1983; **4**: 228–233.
49. Ubeda-Bañon I, Saiz-Sanchez D, de la Rosa-Prieto C, Argandoña-Palacios L, Garcia-Muñozguren S, Martinez-Marcos A. alpha-Synucleinopathy in the human olfactory system in Parkinson's disease: involvement of calcium-binding protein- and substance P-positive cells. *Acta Neuropathol* 2010; **119**: 723–735.

PSYCHOGERIATRICS
The Official Journal of the Japanese Psychogeriatric Society

doi:10.1111/j.1479-8301.2012.00409.x PSYCHOGERIATRICS 2012; 12: 106–114

REVIEW ARTICLE

Molecular imaging of dementia

Takaaki MORI,[1,2] Jun MAEDA,[1] Hitoshi SHIMADA,[1] Makoto HIGUCHI,[1] Hitoshi SHINOTOH,[1] Shu-ichi UENO[2] and Tetsuya SUHARA[1]

[1]Molecular Imaging Center, National Institute of Radiological Sciences, Chiba, and [2]Department of Neuropsychiatry, Neuroscience, Ehime University Graduate School of Medicine, Shitsukawa, Japan

Correspondence: Dr Tetsuya Suhara MD PhD, Molecular Imaging Center, National Institute of Radiological Sciences, 4-9-1 Anagawa, Inage-ku, Chiba 263-8555, Japan. Email: suhara@nirs.go.jp

This review article was presented by the authors in Symposium of the 26th annual meeting of Japanese Psychogeriatrics Society in Tokyo, 15–17 June 2011.

Received 28 September 2011; accepted 19 January 2012.

Abstract

Diagnosis and treatment strategies for dementia are based on the sensitive and specific detection of the incipient neuropathological characteristics, combined with emerging treatments that counteract molecular processes in its pathogenesis. Positron emission tomography (PET) is used for diverse clinical and basic studies on dementia with a wide range of radiotracers. Approaches to visualize amyloid deposition in human brains non-invasively with PET depend on imaging agents reacting with amyloid fibrils. The most widely used tracer is [^{11}C]-6-OH-BTA-1, also known as Pittsburgh Compound-B, which has a high affinity to amyloid β peptide (Aβ) aggregates. Some ^{18}F-labeled amyloid ligands with a longer radioactive half-life have also been developed for broader clinical applications. In addition, there have been demonstrated advantages of tracers with high specific radioactivity in the sensitive detection of amyloid, which have indicated the significance of Aβ-N3-pyroglutamate as a new diagnostic and therapeutic target. Furthermore, beneficial outcomes of Aβ and tau immunization in humans and mouse models have highlighted crucial roles of immunocompetent glia in the protection of neurons against amyloid toxicities. The utility of PET with a radioligand for translocator protein as a biomarker for tau-triggered toxicity, and as a complement to amyloid and tau imaging for diagnostic assessment of tauopathies with and without Aβ pathologies, has also been demonstrated. Meanwhile, brain cholinergic function can be estimated by measuring acetylcholinesterase activity in the brain with PET and radiolabeled acetylcholine analogues. It has been reported that patients with early Parkinson's disease exhibit a reduction in acetylcholinesterase activity in the cerebral cortex, and this decline is more profound in patients with Parkinson's disease with dementia and dementia with Lewy bodies than in patients with Parkinson's disease without dementia. The Alzheimer's Disease Neuroimaging Initiative was a multicentre research project conducted over 6 years that studied changes in cognition, brain structure, and biomarkers in healthy elderly controls and subjects with mild cognitive impairment and Alzheimer's disease. An international workgroup of the National Institute on Aging-Alzheimer's Association has suggested that Alzheimer's disease would be optimally treated before significant cognitive impairment, defined as a 'presymptomatic' or 'preclinical' stage. Therefore, PET will be of technical importance for both clinical and basic research aimed at prodromal pathologies of Alzheimer's disease.

Key words: *Alzheimer's disease (AD), amyloid, Aβ, dementia, microglia, positron emission tomography (PET).*

INTRODUCTION

Japanese society is rapidly ageing, and the increasing number of dementia patients is resulting in social and economic problems. Dementia, progressive cognitive decline with various psychiatric symptoms, leads to a gradually increased restriction of daily activities. About 6% of the population 65 years and older suffers from dementia, and worldwide the number of new

cases in 2000 was estimated to be 4–6 million.[1] Dementia not only affects patients themselves but also places substantial burdens on their caregivers and society, as most patients require long-term care, which can often last 5 years or longer after symptom onset, at their homes or nursing homes. Therefore, a solution to these critical social issues is intimately associated with the establishment of diagnostic and therapeutic approaches to this condition. Alzheimer's disease (AD) is a progressive neurodegenerative disorder characterized by gradual deterioration in cognition and behaviour, and it accounts for about 60% of all cases of dementia. Earlier detection of AD risk would enable preventive and more effective treatment, resulting in a delay in symptom onset that could significantly decrease the prevalence of the disease.[3] This achievement must rely on the sensitive and specific detection of the incipient neuropathological characteristics of AD, combined with emerging treatments that counteract molecular processes in its pathogenesis. Conventional neuroimaging-based measures as exemplified by morphometric indices, regional cerebral blood flow and glucose metabolism have offered informative adjuncts in predicting symptomatic conversion of minor memory disturbance, termed mild cognitive impairment (MCI), to clinically diagnosable AD. Meanwhile, recent advances in molecular imaging research have enabled visualization of brain amyloidosis, the core pathology of AD, potentially allowing diagnosis and initiation of disease-modifying therapies at a presymptomatic stage.

Positron emission tomography (PET) is used for many clinical studies because of its high sensitivity, low invasiveness and quantification capability. Non-invasive assessment of glucose utilization by means of PET with 2-[^{18}F] fluoro-deoxy-glucose has revealed a metabolic deficit in several neurodegenerative disorders, including AD and MCI.[4] Moreover, a broad range of molecular targets can be imaged with various PET tracers in both humans and small animals, owing to flexibility of designing PET probes. In this review, we summarize PET imaging biomarkers applied to research on dementia.

PATHOLOGICAL AND MOLECULAR ETIOLOGY OF ALZHEIMER'S DISEASE

The presence of amyloid lesions, comprised of senile plaques and neurofibrillary tangles, is a neuropathological hallmark of the AD brain.[5] Amyloid β peptide (Aβ) and tau protein constitute plaques and tangles, respectively, and these amyloidogenic molecules have been mechanistically implicated in the pathogenesis of AD and related neurodegenerative dementias. Numerous investigations have supported the notion that cascade reactions of molecular processes triggered by aberrancy of amyloidogenic components involve synaptic loss and neurotransmitter deficits, leading to neuronal death and cognitive impairments. Moreover, studies on the initialization of a neurotoxic cascade by amyloid fibrils have reinforced the rationale for applying *in vivo* amyloid imaging to the detection of AD pathology at an asymptomatic stage. Appearances of amyloid deposits precedent to symptomatic onset have been demonstrated by neuropathological analyses of post-mortem AD brains. As Braak and Braak proposed on the basis of their pathological staging of brain amyloidosis, amyloid deposits spread from the basal neocortex to all cortical regions.[6] In consideration of this putative spatiotemporal profile, the observation that tangles and plaques are already present in widespread areas of preclinical AD brains decisively indicates that the occurrence of amyloid aggregates long precedes cognitive deterioration.[7] In addition to the clinicopathological findings in human subjects, genetically engineered mouse models of familial dementias have provided an insight into the pathophysiological significance of amyloid fibrillogenesis in the devastating effects of AD and other degenerative disorders on neuronal integrities.[8,9] Moreover, studies have also focused on the application of genetically engineered disease models and small animal-dedicated PET devices to the development of amyloid probes and anti-amyloid treatments, as comparative evaluation of multiple candidate tracers and longitudinal assessments of neuropathology can be conducted in the same animals.

AMYLOID IMAGING

Approaches to non-invasive visualization of amyloid deposition in human brains with PET have been based on the development of imaging agents that can efficiently react with amyloid fibrils. The β-pleated sheet is a secondary structure commonly shared by amyloid assemblies, and chemicals that bind to β-sheets would make good candidates for a tracer compound. Thioflavin-S and Congo red are well-known dyes that stain a wide range of amyloid pathologies, and

thioflavin-T is also a chemical capable of binding to amyloid fibrils in a test tube. However, these compounds are not applicable as intravenously administrable tracers for amyloid imaging, as they cannot pass through the blood-brain barrier. Therefore, small and uncharged derivatives of these compounds with blood-brain barrier permeability have been developed as imaging probes, and their radiolabeled versions are used for PET.

With its binding increased in brain areas known to contain both amyloid plaques and neurofibrillary tangles, 2-(1-{6-[(2-[^{18}F]fluoroethyl)(methyl)amino]-2-naphthyl}ethylidene)malononitrile (FDDNP) is the first PET molecular imaging probe successfully applied to *in vivo* visualization of AD pathology in the brain of living patients.[10] However, specific signals of [18F]FDDNP in amyloid-rich regions of AD brains were only 0.3-fold higher than those in the cerebellar reference region. The most widely used amyloid tracer at present is [^{11}C]-6-OH-BTA-1, or Pittsburgh Compound-B (PIB), which was developed by a research group at the University of Pittsburgh (Pittsburgh, PA, USA).[11] [^{11}C]PIB has a favourable combination of a high affinity for Aβ and a moderate log *P*-value of 1.2 (Fig. 1), which accords a high initial uptake to and a fast clearance from non-AD brains. *In vitro* studies have demonstrated a consistency between the amounts of PIB binding sites and biochemically measured Aβ in frontal cortex samples from autopsied AD brains.[12] Since the first report on the successful application of PIB to the differentiation between normal subjects and AD patients, PIB and several other radioligands have been shown to be of great utility for the detection of amyloid at early symptomatic and possibly presymptomatic stages of AD.[13] Indeed, retention of [^{11}C]PIB in the AD neocotex with abundant plaque deposits is 1.5–2-fold higher than that in the cerebellum, much exceeding the performance of [18F]FDDNP. In the first autopsy case report of a patient who underwent an [^{11}C]PIB-PET scan and died 3 months later, a positive correlation between regional patterns of PIB binding and immunohistochemically measured Aβ burden was proven. This study also demonstrated that amyloid deposited as cerebral amyloid angiopathy can be a significant source of radioprobe signals.[14] In a recent study, [^{11}C]AZD2184 was shown to provide higher sensitivity for Aβ amyloid than [^{11}C]PIB,[15] suggesting the capability of this new radioligand in detecting brain amyloidosis at a very early stage. In addition, [^{11}C]-labelled 2-(2-[2-dimethylaminothiazol-5-yl]ethenyl)-6-(2-[fluoro]ethoxy)benzoxazole ([11C]BF-227) was developed and indicated to be a PET probe for *in vivo* detection of dense-cored amyloid deposits in AD patients.[16]

The utility of ^{11}C-labeled tracers is limited by its short radioactive half-life (about 20 min), and they necessitate an on-site production by cyclotron and radiochemistry modules. In contrast, ^{18}F-labeled tracers, with their radioactive half-life of 110 min, can be distributed from a production site to local hospitals running a PET scanner. Given this advantage, [^{18}F]flutemetamol, which is structurally identical to [^{11}C]PIB apart from the presence of [^{18}F]fluorine attached to the core benzene ring, was developed and tested in a phase II clinical trial.[17] In addition, it is reported that florbetaben ([^{18}F]-BAY94-9172),[18] a stilbene derivative with some structural similarities to PIB, has shown high affinity and specificity for Aβ. Also, clinical studies of florbetapir ([^{18}F]AV-45) and [^{18}F]AZD4694 are in progress (Fig. 2).[19,20] A phase III trial for [^{18}F]-BAY94-9172 is ongoing, and data in a clinical trial for [^{18}F]AV-45 were submitted to the US Food and Drug Administration (FDA). In 2008, a FDA advisory committee noted that the detection of amyloid plaque in the brain could have clinical utility. The committee suggested that a new study should use a post-mortem pathological measure as a reference standard and, therefore, be designed to test intra-individual relationships between levels of neuritic amyloid plaques assessed by ante-mortem PET

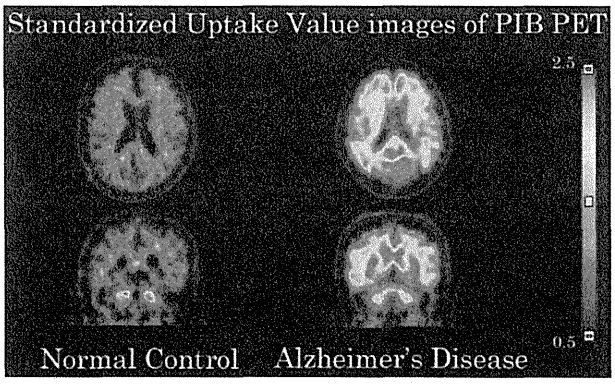

Figure 1 Representative amyloid PET images showing standardized uptake value for PIB. Increased uptake values reflect greater PIB binding in many cortical areas of AD than in normal control. AD, Alzheimer's disease; PET, positron emission tomography; PIB, Pittsburgh Compound-B.

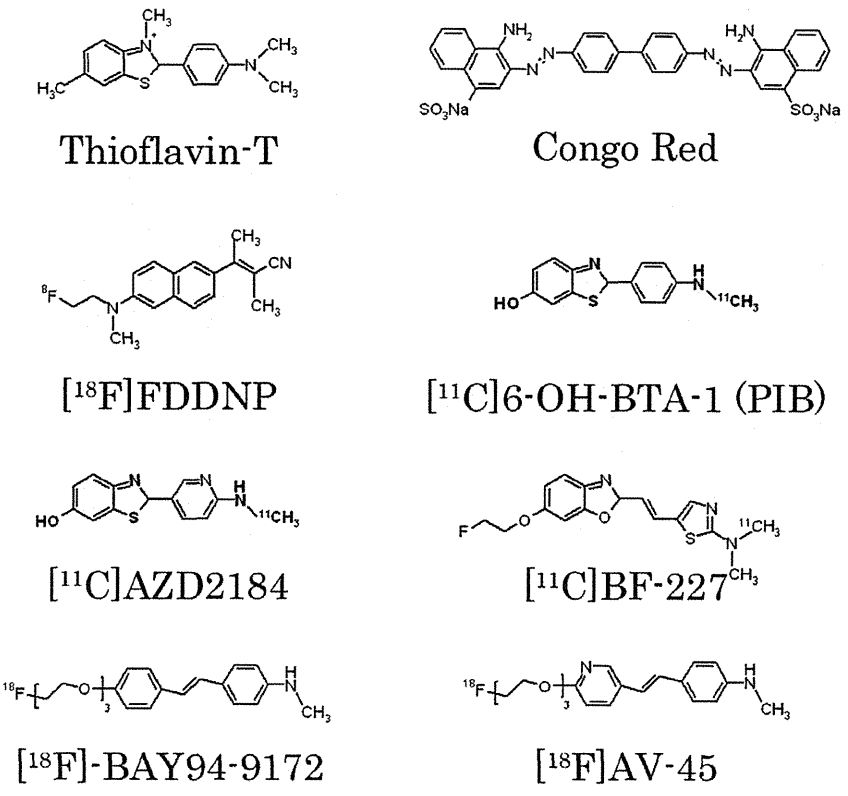

Figure 2 Chemical structures of amyloid ligands. [^{18}F]AV-45, florpiramine; [^{18}F]-BAY94-9172, florbetapir; [^{18}F]FDDNP, 2-(1-{6-[(2-[^{18}F]fluoroethyl)(methyl)amino]-2-naphthyl}ethylidene)malononitrile; PIB, Pittsburgh Compound-B.

imaging and post-mortem histopathology.[21] Following this, in a prospective clinical evaluation conducted from February 2009 through March 2010, [^{18}F]AV-45 PET data were acquired from 35 subjects, including AD patients, and were compared with immunohistochemical and silver stain measures of brain Aβ pathologies after their death. It was demonstrated that [^{18}F]AV-45-PET data was correlated with the presence and density of Aβ lesions.[22]

In contrast to the clinical data on PIB, PET experiments using animal models have not provided unequivocal evidence that radiolabeled compounds administered at an imaging dose bind specifically to brain amyloid, as Aβ plaques were only marginally captured in PET analyses of amyloid precursor protein transgenic (Tg) mouse brains.[23,24] To overcome the insensitivity of amyloid detection in mice, we have recently attempted to use PIB synthesized with high specific radioactivity, which supposedly increased the detectability of non-abundant binding sites, and successfully performed PET visualization of progressively depositing Aβ aggregates in the brains of amyloid precursor protein Tg mice (Fig. 3).[25] In addition, our *in vitro* assays revealed preferential binding of PIB to N-terminally modified Aβ, Aβ-N3-pyroglutamate (Fig. 4).[25] Interestingly, Aβ-N3-pyroglutamate is known to be a major constituent of pathological Aβ deposits in AD brains,[26] is more prone to fibrillization than unmodified Aβ species,[27] and has been critically implicated in Aβ-induced neurotoxicity.[28] These findings possibly support the advantages of tracers with high specific radioactivity in the sensitive detection of mouse amyloid and highlight the significance of Aβ-N3-pyroglutamate as a new diagnostic and therapeutic target that can be specifically monitored by amyloid PET imaging. In the interim, interspecies differences in levels of Aβ-N3-pyroglutamate indicate requirements for the generation of a better mouse model recapitulating AD-characteristic Aβ plaque compositions.[29]

IMAGING OF MICROGLIAL ACTIVATION

It is well known that amyloid deposition triggers microglial and astroglial activation in AD brains.[30] Moreover, beneficial outcomes of Aβ and tau immunization in humans and mouse models have highlighted the

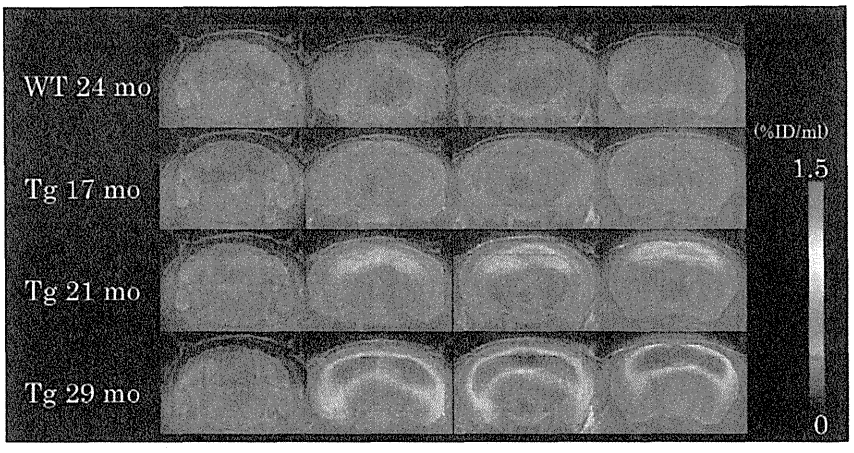

Figure 3 *In vivo* detection of amyloid plaques in wild-type (WT) and APP Tg mice at different ages. PET images were generated by averaging dynamic scan data at 30–60 min after administration of PIB and overlaid on the magnetic resonance imaging template. From left to right, panels represent coronal images at 7, 3, 2 and 0 mm posterior to the bregma. APP, amyloid precursor protein; PET, positron emission tomography; Tg, transgenic.

crucial roles that immunocompetent glia play in protecting neurons against amyloid toxicities.[31] In contrast, our study of tau Tg mice demonstrated attenuated tau accumulation and neuronal loss by suppressing neuroinflammation with an immunosuppressant,[32] suggesting two distinct roles of activated glia involving either detrimental action or protective action on neurons. Upregulation of 18-kDa translocator protein (TSPO), also known as peripheral benzodiazepine receptor, in activated glia is of diagnostic importance in neurological diseases,[33] and several different PET radioligands for this molecule are now available or are under development.[34] Elevated TSPO levels in living AD brains were initially detected with [^{11}C] 1-[2-chlorophenyl]-N-methyl-N-[1-methyl-propyl]-3-isoquinoline carboxamide,[35] and compounds with improved blood-brain barrier permeability and affinity for TSPO, including [^{11}C] N-5-fluoro-2-phenoxyphenyl) -N-(2,5-dimethoxybenzyl)acetamide (DAA1106) and [^{18}F]fluoroethoxy-DAA1106 ([^{18}F]FEDAA1106),[36,37] were developed and applied to neuroimaging of AD patients.[38–40] Autoradiographic assays of model mice with [^{18}F]FEDAA1106 combined with immunohistochemistry have also indicated that microglial TSPO expression is linked to toxic injuries of neurons and may herald neuronal death.[32,41,42] Furthermore, we have developed a novel class of TSPO ligands, [^{11}C] N-benzyl-N-ethyl-2-(7-methyl-8-oxo-2-phenyl-7,8-dihydro-9H-purin-9-yl)acetamide ([11C]AC5216) and its analogues,[43–45] which exhibit faster kinetics in the brain than DAA1106 families. These newer probes potentially produce high-contrast TSPO images and are likely to allow assessment of neurotoxic insults from an early pathogenic stage. Additionally, despite notably enhanced *in vivo* binding of the amyloid radiotracer [^{11}C]PIB, only modest TSPO elevation was observed in aged amyloid precursor protein Tg mice as compared to the tau Tg mice. In these mice, [11C]AC5216 yielded better TSPO contrasts than [^{18}F]FEDAA1106, supporting the possibility of capturing early neurotoxicity with high-performance TSPO probes.[46] An additional line of mouse modelling intraneuronal Aβ accumulation displayed markedly elevated TSPO signals, but this followed noticeable neuronal loss, unlike TSPO upregulation preceding massive neuronal death in tau Tg mice. These data corroborate the utility of TSPO-PET imaging primarily as a biomarker for tau-triggered toxicity and as a complement to amyloid scans for diagnostic assessment of tauopathies with and without Aβ pathologies.[32,47–49] Longitudinal TSPO-PET could also serve to stringently regulate microglial activity within an adequate range during the course of anti-amyloid treatments.

IMAGING OF CHOLINERGIC FUNCTION

Parkinson's disease (PD) is frequently associated with cognitive deficits that can range from subtle deficiencies to dementia.[50] These cognitive deficits are attributed mainly to Lewy body and Lewy neurite pathologies in the cerebral cortex and limbic structures, and partly to AD-type pathology in the forebrain and to the core PD pathology in the substantia nigra and brainstem. Alterations of ascending cholinergic systems from the basal forebrain and the brainstem have been implicated as pivotal players in cognitive

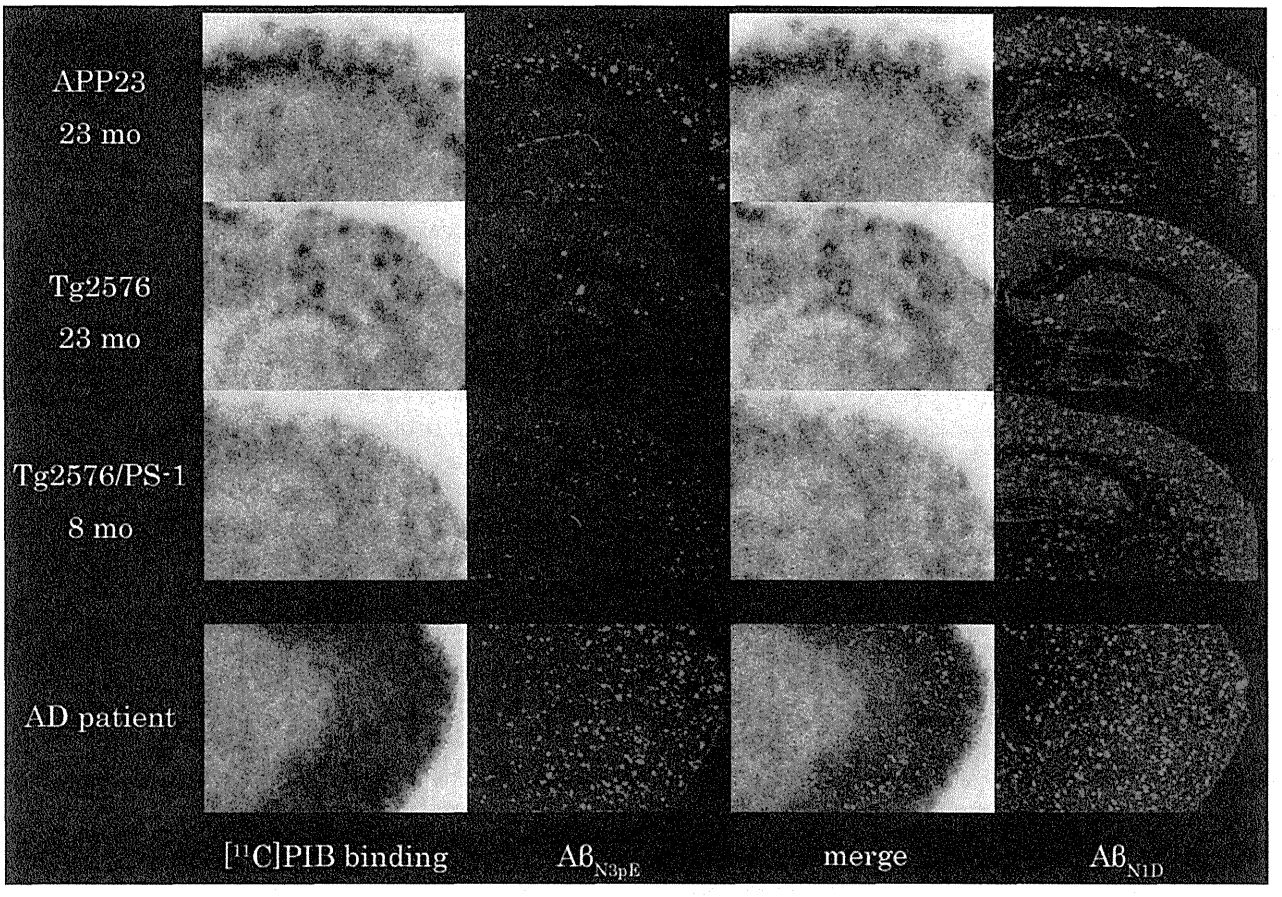

Figure 4 Search for Aβ subtypes accumulating in close relation to [^{11}C]PIB binding sites and association between *in vitro* radiolabelling of amyloid with [^{11}C]PIB and N-terminal truncation/modification of Aβ. Brain sections from a 23-month-old APP23 mouse (top row), 23-month-old Tg2576 mouse (second row), 8-month-old presenilin-1(PS-1)/APP double Tg mouse (third row), and AD patient (bottom row) were used for autoradiography with [^{11}C]PIB (autoradiograms are shown in the first column to the left), which were then immunostained with a polyclonal antibody against Aβ-N3-pyroglutamate ($Aβ_{N3pE}$) (second column). Co-localization of PIB radiolabelling with $Aβ_{N3pE}$ deposition was assessed by merging autoradiograms with immunohistochemical data (third column). Sub-adjacent sections were also immunolabeled with a polyclonal antibody against N-terminally unmodified Aβ, $Aβ_{N1D}$ (fourth column). Aβ, amyloid β peptide; AD, Alzheimer's disease; APP, amyloid precursor protein; PIB, Pittsburgh Compound-B; Tg, transgenic.

dysfunctions, especially impaired attention and consciousness.[51] Loss of cholinergic neurons in the nucleus basalis of Mynert has been observed in postmortem PD brains and has been thought to contribute to cognitive decline in PD.[52] PD and dementia with Lewy bodies (DLB) are regarded as two ends of the spectrum of Lewy body disease. Cholinergic deficits may play a role in these diseases, and widespread and profound reduction of choline acetyltransferase (AChE) activity has been observed in postmortem brains with DLB. Brain cholinergic function can be assayed by measuring AChE activity in the brain with PET and radiolabeled acetylcholine analogues as exemplified by N-[^{11}C]-methyl-4-piperidyl acetate ([11C]MP4A) and N-[^{11}C]-methyl-4-piperidyl propionate.[53–55] Some PET studies showed a significant reduction in cortical AChE activity in PD,[56,57] and this decrease was more sizeable in PD with dementia and DLB than in AD. Using [11C]MP4A, we demonstrated that an early PD group exhibited a reduction in AChE activity in the cerebral cortex, particularly in the medial occipital cortex. Moreover, we revealed that the widespread and pronounced reduction of AChE activity in the cerebral cortices, particularly in the posterior cortical regions, in patients with PD with dementia and DLB. The decline in cerebral cortical

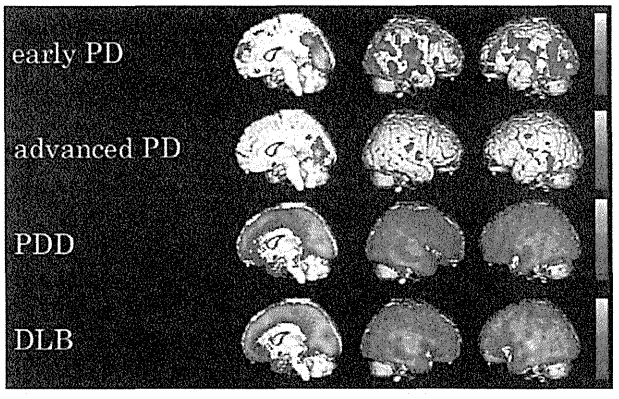

Figure 5 Regions showing a reduction in k^3, a rate constant for AChE activity, observed in early-stage PD, advanced-stage PD, PDD, and DLB, compared with healthy controls. The white-to-blue colour gradient indicates the locations and magnitude of the decrease in k^3 values. AChE, acetyltransferase; DLB, dementia with Lewy bodies; PD, Parkinson's disease; PDD, Parkinson's disease with dementia.

AChE activity was more profound in PD with dementia/DLB patients than in PD patients without dementia (Fig. 5).[58] We also found that cerebral cortical AChE activity was moderately reduced in corticobasal syndrome and mildly reduced in progressive supranuclear palsy, while thalamic AChE activity was remarkably reduced only in supranuclear palsy. Unlike these illnesses, there was no AChE activity deficit in the cerebral cortex and thalamus of patients with frontotemporal dementia.[59,60] In AD patients, reduced AChE activity after treatment with donepezil was shown in our PET study with [11C]MP4A,[61] implying potential usefulness of cholinergic PET imaging for evaluation of symptomatic treatments for dementia.

THE ALZHEIMER'S DISEASE NEUROIMAGING INITIATIVE (ADNI)

The ADNI, initiated in October 2004, was a 6-year research project focusing on studies of changes in cognition, brain structure and biomarkers in cognitively healthy elderly and subjects with MCI and AD. This project was aimed at determining and validating standardized protocols of magnetic resonance imaging, PET imaging and cerebrospinal fluid/blood biomarker measurements, and evaluating outputs of these assays as predictors of disease onset and progression and outcomes in future clinical trials of anti-AD treatments in the USA (http://adni.loni.ucla.edu/). One report in this study demonstrated that a decline in episodic memory may be mechanistically associated with Aβ-induced hippocampal atrophy in PIB-positive MCI subjects and even in cognitively normal elderly individuals, strengthening the implication that levels of PIB uptake in non-demented populations is biologically meaningful.[62] Another arm of the study reported a dissociation between the rate of amyloid deposition and the rate of neurodegeneration late in life, with amyloid deposition proceeding at a constant slow rate while neurodegeneration accelerates; this section also reported that clinical symptoms are coupled to neurodegeneration but not amyloid deposition.[63] Moreover, this project suggested that the earliest detectable changes are those related to Aβ, as detected by cerebrospinal fluid tests and amyloid PET imaging. The establishment of the ADNI stimulated many other related efforts, including the Japanese ADNI (http://www.j-adni.org/), which was started as a part of the worldwide ADNI.

PRECLINICAL STAGES OF AD

On the basis of the above-mentioned evidence, the use of AD-specific biomarkers for *in vivo* staging of the disease has been proposed.[64] These biomarkers exhibit abnormality in a temporally ordered manner as the disease progresses. Changes in Aβ-related biomarkers, such as cerebrospinal fluid Aβ42 and amyloid PET imaging, become prominent before the appearance of clinical symptoms and nearly reach a plateau by the time clinical symptoms emerge.[64] In addition, an international workgroup of the National Institute on Aging-Alzheimer's Association suggested that AD should be optimally treated at a 'presymptomatic' or 'preclinical' stage before the occurrence of significant cognitive impairments.[65] It is possible that individuals with abnormal biomarker levels already develop initial neurodegeneration, and amyloid-modifying therapies may be less efficacious after the downstream pathological process is set in motion.

CONCLUSION

We have reviewed molecular imaging research on dementia by focusing on PET studies. Establishment of radiolabeled tracers optimized for *in vivo* imaging of Aβ plaques could permit pathology-based diagnosis of AD at an asymptomatic stage and allow early immunotherapeutic intervention. Imaging agents for microglial activation and cholinergic function are also useful

research tools, and thus, PET will be in even greater demand as a clinical and basic research technology.

REFERENCES

1 Wimo A, Winblad B, Aguero-Torres H, von Strauss E. The magnitude of dementia occurrence in the world. *Alzheimer Dis Assoc Disord* 2003; **17**: 63–67.
2 Khachaturian ZS. Diagnosis of Alzheimer's disease. *Arch Neurol* 1985; **42**: 1097–1105.
3 DeKosky ST, Marek K. Looking backward to move forward: early detection of neurodegenerative disorders. *Science* 2003; **302**: 830–834.
4 Drzezga A, Grimmer T, Riemenschneider M *et al*. Prediction of individual clinical outcome in MCI by means of genetic assessment and (18)F-FDG PET. *J Nucl Med* 2005; **46**: 1625–1632.
5 Higuchi M, Lee VMY, Trojanowski JQ. Pathobiological features in neurodegenerative diseases: an overview. In: Numura Y, Takeda T, Okuma Y, eds. *International Congress Series 1260: The Senescence-Accelerated Mouse (SAM): An Animal Model of Senescence*. Amsterdam: Elsevier, 2004; 69–75.
6 Braak H, Braak E. Neuropathological staging of Alzheiner-related changes. *Acta Neuropathol* 1991; **82**: 239–259.
7 Price JL, Morris JC. Tangles and plaques in nondemented aging and 'preclinical' Alzheimer's disease. *Ann Neurol* 1999; **45**: 358–368.
8 Higuchi M, Ishihara T, Zhang B *et al*. Transgenic mouse model of tauopathies with glial pathology and nervous system degeneration. *Neuron* 2002; **35**: 433–446.
9 Higuchi M, Lee VM, Trojanowski JQ. Tau and axonopathy in neurodegenerative disorders. *Neuromolecular Med* 2002; **2**: 131–150.
10 Small GW, Kepe V, Ercoli LM *et al*. PET of brain amyloid and tau in mild cognitive impairment. *N Engl J Med* 2006; **355**: 2652–2663.
11 Klunk WE, Engler H, Nordberg A *et al*. Imaging brain amyloid in Alzheimer's disease with Pittsburgh Compound-B. *Ann Neurol* 2004; **55**: 306–319.
12 Näslund J, Haroutunian V, Mohs R *et al*. Correlation between elevated levels of amyloid beta-peptide in the brain and cognitive decline. *JAMA* 2000; **283**: 1571–1577.
13 Mintun MA, Larossa GN, Sheline YI *et al*. [11C]PIB in a nondemented population: potential antecedent marker of Alzheimer disease. *Neurology* 2006; **67**: 446–452.
14 Bacskai BJ, Frosch MP, Freeman SH *et al*. Molecular imaging with Pittsburgh Compound B confirmed at autopsy: a case report. *Arch Neurol* 2007; **64**: 431–434.
15 Johnson AE, Jeppsson F, Sandell J *et al*. AZD2184: a radioligand for sensitive detection of beta-amyloid deposits. *J Neurochem* 2009; **108**: 1177–1186.
16 Kudo Y, Okamura N, Furumoto S *et al*. 2-(2-[2-Dimethylaminothiazol-5-yl]ethenyl)-6-(2-[fluoro]ethoxy) benzoxazole: a novel PET agent for *in vivo* detection of dense amyloid plaques in Alzheimer's disease patients. *J Nucl Med* 2007; **48**: 553–561.
17 Vandenberghe R, Van Laere K, Ivanoiu A *et al*. 18F-flutemetamol amyloid imaging in Alzheimer disease and mild cognitive impairment: a phase 2 trial. *Ann Neurol* 2010; **68**: 319–329.
18 Rowe CC, Ackerman U, Browne W *et al*. Imaging of amyloid beta in Alzheimer's disease with 18F-BAY94-9172, a novel PET tracer: proof of mechanism. *Lancet Neurol* 2008; **7**: 129–135.
19 Choi SR, Golding G, Zhuang Z *et al*. Preclinical properties of 18F-AV-45: a PET agent for Abeta plaques in the brain. *J Nucl Med* 2009; **50**: 1887–1894.
20 Juréus A, Swahn BM, Sandell J *et al*. Characterization of AZD4694, a novel fluorinated Abeta plaque neuroimaging PET radioligand. *J Neurochem* 2010; **114**: 784–794.
21 Avid Radiopharmaceuticals, Inc. FDA Advisory Committee Meeting. October 23, 2008. 18F-AV-45: PET Amyloid Plaque Imaging Agent Summary of Development Program and Proposed Phase III Plan. http://www.fda.gov/ohrms/dockets/ac/08/briefing/2008-4382b1-02-Avid.pdf.
22 Clark CM, Schneider JA, Bedell BJ *et al*. Use of florbetapir-PET for imaging beta-amyloid pathology. *JAMA* 2011; **305**: 275–283.
23 Klunk WE, Lopresti BJ, Ikonomovic MD *et al*. Binding of the positron emission tomography tracer Pittsburgh compound-B reflects the amount of amyloid-beta in Alzheimer's disease brain but not in transgenic mouse brain. *J Neurosci* 2005; **25**: 10598–10606.
24 Toyama H, Ye D, Ichise M *et al*. PET imaging of brain with the beta-amyloid probe, [11C]6-OH-BTA-1, in a transgenic mouse model of Alzheimer's disease. *Eur J Nucl Med Mol Imaging* 2005; **32**: 593–600.
25 Maeda J, Higuchi M, Inaji M *et al*. Phase-dependent roles of reactive microglia and astrocytes in nervous system injury as delineated by imaging of peripheral benzodiazepine receptor. *Brain Res* 2007; **1157**: 100–111.
26 Saido TC, Iwatsubo T, Mann DM, Shimada H, Ihara Y, Kawashima S. Dominant and differential deposition of distinct beta-amyloid peptide species, A beta N3(pE), in senile plaques. *Neuron* 1995; **14**: 457–466.
27 Schilling S, Lauber T, Schaupp M *et al*. On the seeding and oligomerization of pGlu-amyloid peptides (*in vitro*). *Biochemistry* 2006; **45**: 12393–12399.
28 Wirths O, Weis J, Kayed R, Saido TC, Bayer TA. Age-dependent axonal degeneration in an Alzheimer mouse model. *Neurobiol Aging* 2007; **28**: 1689–1699.
29 Kawarabayashi T, Younkin LH, Saido TC, Shoji M, Ashe KH, Younkin SG. Age-dependent changes in brain, CSF, and plasma amyloid (beta) protein in the Tg2576 transgenic mouse model of Alzheimer's disease. *J Neurosci* 2001; **21**: 372–381.
30 McGeer PL, McGeer EG. The inflammatory response system of brain: implications for therapy of Alzheimer and other neurodegenerative diseases. *Brain Res Brain Res Rev* 1995; **21**: 195–218.
31 Asuni AA, Boutajangout A, Quartermain D, Sigurdsson EM. Immunotherapy targeting pathological tau conformers in a tangle mouse model reduces brain pathology with associated functional improvements. *J Neurosci* 2007; **27**: 9115–9129.
32 Yoshiyama Y, Higuchi M, Zhang B *et al*. Synapse loss and microglial activation precede tangles in a P301S tauopathy mouse model. *Neuron* 2007; **53**: 337–351.
33 Diorio D, Welner SA, Butterworth RF, Meaney MJ, Suranyi-Cadotte BE. Peripheral benzodiazepine binding sites in Alzheimer's disease frontal and temporal cortex. *Neurobiol Aging* 1991; **12**: 255–258.
34 Miyoshi M, Ito H, Arakawa R *et al*. Quantitative analysis of peripheral benzodiazepine receptor in the human brain using PET with (11)C-AC-5216. *J Nucl Med* 2009; **50**: 1095–1101.
35 Cagnin A, Brooks DJ, Kennedy AM *et al*. In-vivo measurement of activated microglia in dementia. *Lancet* 2001; **358**: 461–467.
36 Maeda J, Suhara T, Zhang MR *et al*. Novel peripheral benzodiazepine receptor ligand [11C]DAA1106 for PET: an imaging tool for glial cells in the brain. *Synapse* 2004; **52**: 283–291.

37 Zhang MR, Maeda J, Ogawa M *et al.* Development of a new radioligand, N-(5-fluoro-2-phenoxyphenyl)-N-(2-[18F] fluoroethyl-5-methoxybenzyl)acetamide, for pet imaging of peripheral benzodiazepine receptor in primate brain. *J Med Chem* 2004; **47**: 2228–2235.
38 Yasuno F, Ota M, Kosaka J *et al.* Increased binding of peripheral benzodiazepine receptor in Alzheimer's disease measured by positron emission tomography with [11C]DAA1106. *Biol Psychiatry* 2008; **64**: 835–841.
39 Maeda J, Ji B, Irie T *et al.* Longitudinal, quantitative assessment of amyloid, neuroinflammation, and anti-amyloid treatment in a living mouse model of Alzheimer's disease enabled by positron emission tomography. *J Neurosci* 2007; **27**: 10957–10968.
40 Venneti S, Lopresti BJ, Wang G *et al.* A comparison of the high-affinity peripheral benzodiazepine receptor ligands DAA1106 and (R)-PK11195 in rat models of neuroinflammation: implications for PET imaging of microglial activation. *J Neurochem* 2007; **102**: 2118–2131.
41 Ji B, Maeda J, Sawada M *et al.* Imaging of peripheral benzodiazepine receptor expression as biomarkers of detrimental versus beneficial glial responses in mouse models of Alzheimer's and other CNS pathologies. *J Neurosci* 2008; **28**: 12255–12267.
42 Gulyás B, Makkai B, Kása P *et al.* A comparative autoradiography study in post mortem whole hemisphere human brain slices taken from Alzheimer patients and age-matched controls using two radiolabelled DAA1106 analogues with high affinity to the peripheral benzodiazepine receptor (PBR) system. *Neurochem Int* 2009; **54**: 28–36.
43 Zhang MR, Kumata K, Maeda J *et al.* 11C-AC-5216: a novel PET ligand for peripheral benzodiazepine receptors in the primate brain. *J Nucl Med* 2007; **48**: 853–861.
44 Yanamoto K, Kumata K, Yamasaki T *et al.* [18F]FEAC and [18F]FEDAC: two novel positron emission tomography ligands for peripheral-type benzodiazepine receptor in the brain. *Bioorg Med Chem Lett* 2009; **19**: 1707–1710.
45 Yanamoto K, Yamasaki T, Kumata K *et al.* Evaluation of N-benzyl-N-[11C]methyl-2-(7-methyl-8-oxo-2-phenyl-7,8-dihydro-9H-purin-9-yl)acetamide ([11C]DAC) as a novel translocator protein (18 kDa) radioligand in kainic acid-lesioned rat. *Synapse* 2009; **63**: 961–971.
46 Maeda J, Zhang MR, Okauchi T *et al.* In vivo positron emission tomographic imaging of glial responses to amyloid-beta and tau pathologies in mouse models of Alzheimer's disease and related disorders. *J Neurosci* 2011; **31**: 4720–4730.
47 Miyoshi M, Shinotoh H, Wszolek ZK *et al.* In vivo detection of neuropathologic changes in presymptomatic MAPT mutation carriers: a PET and MRI study. *Parkinsonism Relat Disord* 2010; **16**: 404–408.
48 Higuchi M, Saido TC, Suhara T. Animal models of tauopathies. *Neuropathology* 2006; **26**: 491–497.
49 Higuchi M, Maeda J, Ji B *et al.* In-vivo visualization of key molecular processes involved in Alzheimer's disease pathogenesis: insights from neuroimaging research in humans and rodent models. *Biochim Biophys Acta* 2010; **1802**: 373–388.
50 Emre M, Aarsland D, Brown R *et al.* Clinical diagnostic criteria for dementia associated with Parkinson's disease. *Mov Disord* 2007; **22**: 1689–1707.
51 Bartus RT, Dean RL 3rd, Beer B, Lippa AS. The cholinergic hypothesis of geriatric memory dysfunction. *Science* 1982; **217**: 408–414.
52 Asahina M, Shinotoh H, Hirayama K *et al.* Hypersensitivity of cortical muscarinic receptors in Parkinson's disease demonstrated by PET. *Acta Neurol Scand* 1995; **91**: 437–443.
53 Namba H, Iyo M, Fukushi K *et al.* Human cerebral acetylcholinesterase activity measured with positron emission tomography: procedure, normal values and effect of age. *Eur J Nucl Med* 1999; **26**: 135–143.
54 Iyo M, Namba H, Fukushi K *et al.* Measurement of acetylcholinesterase by positron emission tomography in the brains of healthy controls and patients with Alzheimer's disease. *Lancet* 1997; **349**: 1805–1809.
55 Kuhl DE, Koeppe RA, Minoshima S *et al.* In vivo mapping of cerebral acetylcholinesterase activity in aging and Alzheimer's disease. *Neurology* 1999; **52**: 691–699.
56 Shinotoh H, Namba H, Yamaguchi M *et al.* Positron emission tomographic measurement of acetylcholinesterase activity reveals differential loss of ascending cholinergic systems in Parkinson's disease and progressive supranuclear palsy. *Ann Neurol* 1999; **46**: 62–69.
57 Bohnen NI, Kaufer DI, Ivanco LS *et al.* Cortical cholinergic function is more severely affected in parkinsonian dementia than in Alzheimer disease: an *in vivo* positron emission tomographic study. *Arch Neurol* 2003; **60**: 1745–1748.
58 Shimada H, Hirano S, Shinotoh H *et al.* Mapping of brain acetylcholinesterase alterations in Lewy body disease by PET. *Neurology* 2009; **73**: 273–278.
59 Hirano S, Shinotoh H, Shimada H *et al.* Cholinergic imaging in corticobasal syndrome, progressive supranuclear palsy and frontotemporal dementia. *Brain* 2010; **133**: 2058–2068.
60 Hirano S, Eckert T, Flanagan T, Eidelberg D. Metabolic networks for assessment of therapy and diagnosis in Parkinson's disease. *Mov Disord* 2009; **24**: 725–731.
61 Ota T, Shinotoh H, Fukushi K *et al.* Estimation of plasma IC50 of donepezil for cerebral acetylcholinesterase inhibition in patients with Alzheimer disease using positron emission tomography. *Clin Neuropharmacol* 2010; **33**: 74–78.
62 Mormino EC, Kluth JT, Madison CM *et al.* Episodic memory loss is related to hippocampal-mediated beta-amyloid deposition in elderly subjects. *Brain* 2009; **132**: 1310–1323.
63 Jack CR Jr, Lowe VJ, Weigand SD *et al.* Serial PIB and MRI in normal, mild cognitive impairment and Alzheimer's disease: implications for sequence of pathological events in Alzheimer's disease. *Brain* 2009; **132**: 1355–1365.
64 Jack CR Jr, Knopman DS, Jagust WJ *et al.* Hypothetical model of dynamic biomarkers of the Alzheimer's pathological cascade. *Lancet Neurol* 2010; **9**: 119–128.
65 Sperling RA, Aisen PS, Beckett LA *et al.* Toward defining the preclinical stages of Alzheimer's disease: recommendations from the National Institute on Aging-Alzheimer's Association workgroups on diagnostic guidelines for Alzheimer's disease. *Alzheimers Dement* 2011; **7**: 280–292.

Rev. Neurosci., Vol. 23(3): 263–268, 2012 • Copyright © by Walter de Gruyter • Berlin • Boston. DOI 10.1515/revneuro-2012-0029

A review of the default mode network in aging and dementia based on molecular imaging

Yasuomi Ouchi[1,*] and Mitsuru Kikuchi[2]

[1]Department of Biofunctional Imaging, Medical Photonics Research Center, Hamamatsu University School of Medicine, Hamamatsu 431-3192, Japan
[2]Research Center for Child Mental Development, Graduate School of Medical Science, Kanazawa University, Kanazawa 920-8641, Japan

*Corresponding author
e-mail: ouchi@hama-med.ac.jp

Abstract

The default mode network (DMN) is a unique idea that attracts many neuroimaging researchers to examine alterations in the resting-state brain physiology in normal aging and psychiatric and neurological disorders predominantly by using functional magnetic resonance imaging (fMRI). In dementias, especially in Alzheimer's disease (AD), one of the recent topics in an imaging domain is depicting its pathological substance, β-amyloid protein (Aβ) *in vivo* using positron emission tomography (PET). This Aβ accumulation was not only discovered in AD but also frequently in cognitively normal people. Indeed, there is evidence that subjects with high Aβ deposition tend to be considered as those who are very likely to develop AD in the future. Recent reports also show that the DMN in AD patients is affected in conjunction with Aβ deposition. Our recent study of the cognitive and physiological impact of Aβ accumulation on the DMN function in normal elderly people using PET has shown that the amount of Aβ deposits is negatively correlated with the DMN function, and the lower function of the DMN is associated with poorer working memory performance. As expected, Aβ deposition in the brain, however minute the degree of its accumulation can be, may cause neuronal discoordination in the DMN along with poor working memory in normal aging. As literature on fMRI-based DMN activity is profuse, here, we discuss the pathophysiological aspect of the DMN from a molecular imaging viewpoint.

Keywords: amyloid deposition; default mode network; glucose metabolism; neurotransmitter; positron emission tomography.

Introduction

After the advent of a new concept on deactivation during task-induced brain activity coined as the 'default mode network (DMN)' (Raichle et al., 2001), the DMN has still been a hot topic among brain mappers who try to extract a surrogate marker that can characterize disease entities from brain images. Indeed, recent reports on the DMN are flourishing in research of aging and dementia and are fairly informative for investigators interested in the DMN (Greicius et al., 2004; Damoiseaux et al., 2008; van den Heuvel et al., 2008; Sambataro et al., 2010; Zhou et al., 2010; Jones et al., 2011; Tomasi and Volkow 2011). This trend may be propelled by the fact that the DMN covers brain regions vulnerable to structural atrophy and metabolic reduction along with β-amyloid protein (Aβ) deposition (Minoshima et al., 1997; Greicius et al., 2004; Sperling et al., 2009; Sheline et al., 2010; Lehmann et al., 2012). Alterations in the DMN exist along a continuum from normal aging to mild cognitive impairment (MCI) and to Alzheimer's disease (AD). Even among cognitively normal subjects, reduction in the DMN function is also seen in subjects with APOE-ε4 carriers (Machulda et al., 2011; Westlye et al., 2011). With an easy accessibility and no radiation exposure, the DMN study with functional magnetic resonance imaging (fMRI) is indeed a useful tool for depicting abnormalities in the DMN in patients with these types of neurological disorders. In particular, a recent technique based on independent principal component analysis using fMRI resting-state signals allow researchers to extend the study domain from adults to children (Thomason et al., 2008). This data-driven approach where coactivated brain regions are mapped according to temporal correlations in the resting-state brain activity may have its own merit, but it is uncertain if examinees are really under the 'resting' condition. In contrast to this approach, a seed-based method according to *a priori* information in conjunction with resting and task-induced scan acquisition may mitigate such critics about the condition factors, at rest or at exercise. With these fMRI methods, fMRI on the DMN would possibly become a computer-guided diagnostic tool in the future.

However, the reality is not so easy because fMRI only depicts functional connectivity between voxels and it is unclear how disruptions in the connectivity account for the pathological process or neuronal damages. Thus, a multimodal approach is necessary to elucidate the pathophysiological progresses in the DMN in aging and dementia. In this review, we focus on different issues from previous DMN reports viewed from the temporal characteristics of fMRI blood oxygen level-dependent (BOLD) signals and discuss abnormalities of neuronal metabolism, Aβ burden along with neuroinflammation and neurotransmitter systems in the DMN of normal elderly and patients with AD, based on molecular imaging.

Cerebral metabolism

Anatomically, the DMN consists of brain regions including the posterior cingulate cortex (PCC), precuneus, medial prefrontal

and inferolateral parietal cortices, medial temporal cortex, all of which are functionally connected in the resting state. Specifically, the PCC in the resting-state activity is more significant in dementia because of the prominence of abnormal activity in AD (Greicius et al., 2004; Buckner et al., 2005). PET shows that the PCC has the highest level of metabolism in humans (Andreasen et al., 1995; Minoshima et al., 1997), and it was confirmed by monkey studies that the PCC (including the retrosplenial region) and anterior thalamus had the highest level of glucose metabolism (Vogt and Laureys, 2005) and cytochrome *c* oxidase activity (Carroll and Wong-Riley, 1984). This oxidase is a mitochondrial enzyme for oxidative phosphorylation and its density reflects the density of mitochondria. It was also shown that the anterior cingulate cortex (ACC), a part of the DMN, contains 40% of enzymatic activity of the PCC. Because the PCC receives axonal projections from the anterior thalamic nuclei, thalamic lesions result in reduced activity of this enzyme in the rat retrosplenial region (Vogt and Laureys, 2005). In addition, the midbrain reticular formation projecting to the anteroventral thalamic nuclei involves maintenance of wakefulness (Kinomura et al., 1996; Steriade, 1996). Thus, the anterior thalamus and brainstem system probably drive the PCC metabolism.

From a functional point of view, the PCC in the DMN involving high-level cognitive functions plays a central role in emotion and anxiety during tasks (Maddock et al., 2003) and autobiographical episodic memory and self-referential processing (Kjaer et al., 2002; D'Argembeau et al., 2005; Ries et al., 2006). PCC activity is strongly coupled with increased activity in the medical frontal cortex (subgenual cingulate) and decreased activity in the lateral prefrontal cortex (Greicius et al., 2003). This coupling may be disrupted in aging because there is a difficulty in switching from a default mode to a task-induced mode of brain activation in older subjects (Grady et al., 2006). In our recent study, we used this concept and expressed a degree of the functional coupling between medial frontoparietal regions as a similarity index (Figure 1A) and found that this index was well correlated to the posterior part of parietotemporal region consisting of the DMN in cognitively normal elderly people (Figure 1B) (Kikuchi et al., 2011). In AD, however, the metabolism of these regions is significantly reduced as seen in our sensitivity map for AD (Figure 2), in which the darker color of sensitivity indicates greater likelihood of AD pathophysiology (Kakimoto et al., 2011). This sensitivity map also suggests that the gray area represents the DMN well.

β-Amyloid deposition and inflammation

Accumulation of Aβ is important in the pathology of AD because this process is responsible for triggering tau phosphorylation and neurofibrillary tangle formation, which lead to neurodegeneration in AD (Hardy and Selkoe, 2002). Recent PET imaging studies showed that the DMN function was impaired in AD patients and altered in healthy elderly people by some degree of Aβ deposition (Greicius et al., 2004; Hedden et al., 2009; Sperling et al., 2009; Sheline et al., 2010; Kikuchi et al., 2011). As shown in our recent study, Pittsburgh Compound-B (PIB) accumulation in the whole cerebral cortex (medial frontal, middle temporal and inferior temporal cortices) showed a negative correlation with the similarity index in the DMN (Figure 3) (Kikuchi et al., 2011). This indicates that the functional coupling of medial frontoposterior DMN seems to be disrupted by Aβ deposition in the DMN along with deterioration of cognitive performance in normal aging. These lines of evidence on Aβ deposition measured by PET with [^{11}C]PIB confirm that [^{11}C]PIB uptake can be a surrogate biomarker for brain functional deterioration during the preclinical state of Aβ pathology. This preclinical significance of Aβ deposition cannot be recognized after diagnosis of AD as shown in previous studies. Total amount of Aβ deposition did not correlate with disease progression in histologically proven AD patients (Lue et al., 1999; McLean et al., 1999),

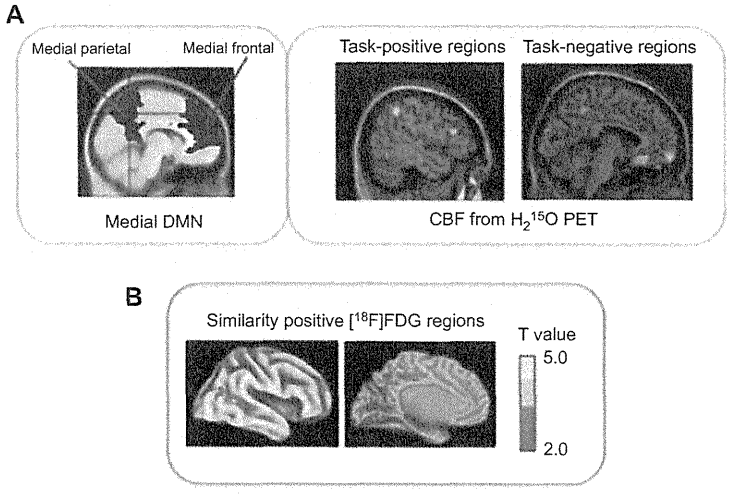

Figure 1 Functional coupling in the medial frontoparietal region.
(A) Default mode network in the similarity of CBF response in the resting condition between medial frontal and parietal cortices. (B) Positive correlation of [^{18}F]FDG uptake in the temporoparietal cortex with the similarity index. Modified from Kikuchi et al. (2011).

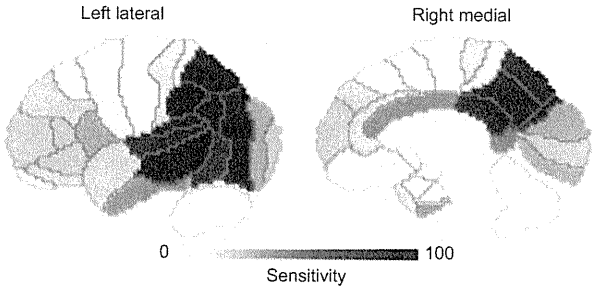

Figure 2 Sensitivity distribution maps of Brodmann areas with different black-and-white colors that denote the levels of sensitivity to differentiate Alzheimer's disease.
Modified from Kakimoto et al. (2011).

and in probable AD patients there was no significant association between [^{11}C]PIB uptake and cognitive deterioration or clinical severity (Rowe et al., 2007; Yokokura et al., 2010), or only a weak association (Pike et al., 2007). This [^{11}C]PIB accumulation seemed to reach a plateau at the level of dementia with moderate clinical severity (i.e., sum of the individual ratings of CDR >0.5) (Grimmer et al., 2009). In any case, it is easy to expect that the presence of Aβ accumulation as highlighted in the DMN is a sign of disruption of harmonization of the neuronal functions.

This contention is supported by the fact that Aβ accumulation activates microglia in the brain (Tan et al., 2002; Wyss-Coray, 2006), and the activated microglia in turn accelerate Aβ accumulation by releasing proinflammatory neurotoxic substances (Chen et al., 2006; Tahara et al., 2006; Richard et al., 2008). Microglia are involved in immune surveillance in the intact brain and become activated in response to inflammation, trauma, ischemia, tumor and neurodegeneration (Kreutzberg, 1996). In the AD brain, the region of increased microglial activity probably accompanies cerebral glucose hypometabolism and a higher rate of brain atrophy, suggesting that the degree of microglial activation predicts disease progression in AD (Cagnin et al., 2001). Our previous

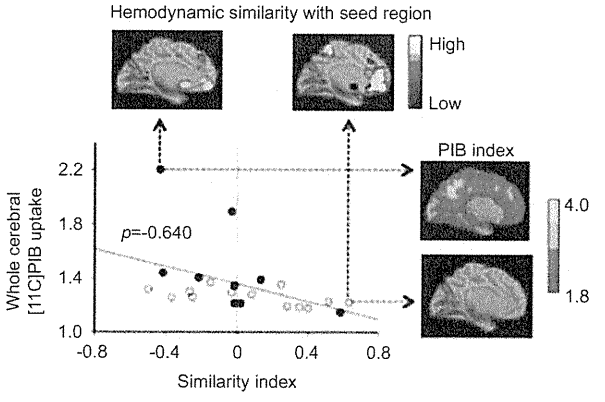

Figure 3 Spearman's rank correlation analysis between adjusted regional [^{11}C]PIB uptake and the similarity index.
Modified from Kikuchi et al. (2011).

PET study with [^{11}C] (*R*)PK11195 for activated microglia, [^{11}C]PIB for Aβ deposition and [^{18}F]FDG for glucose metabolism confirmed this pathological-inflammatory event in the living AD brain (Yokokura et al., 2010). We showed a significant increase in [^{11}C](*R*)PK11195 binding in the ACC and PCC, where there was a more robust increase in [^{11}C] PIB accumulation and marked decrease in [^{18}F]FDG uptake (Figure 4). The distribution of activated microglia is similar in the medial side of the DMN, suggesting that the higher level of energy metabolism at the resting state (DMN) may be vulnerable to any pathological event as seen in AD. Interestingly, direct comparisons between [^{11}C](*R*)PK11195 and [^{11}C]PIB binding showed a significant negative correlation between these two parameters (Yokokura et al., 2010). This indicates that Aβ accumulation shown by [^{11}C]PIB is not always the primary cause of microglial activation, but rather the negative correlation observed in the PCC suggests that microglia can show higher activation during the production of Aβ in early AD or can clear the accumulated Aβ fibrils away from the devastated brain environment at the later stage. In this pathology, one of the soluble oligomer amyloid species is considered to be a more powerful pathogen than the insoluble Aβ fibrils in AD (Montalto et al., 2007). In human studies, increased soluble Aβ levels in the AD cerebral cortices were highly correlated with disease severity (Lue et al., 1999; McLean et al., 1999). As [^{11}C]PIB cannot distinguish insoluble from soluble Aβ (Klunk et al., 2004), it is not currently known how much soluble Aβ harms the brain *in vivo* directly. However, the present observations may support the suggestion that soluble Aβ (oligomer) depicted partly by [^{11}C]PIB plays a central role in cognitive deterioration in the elderly. As people get old, the DMN function deteriorates. If these poisonous Aβ oligomers

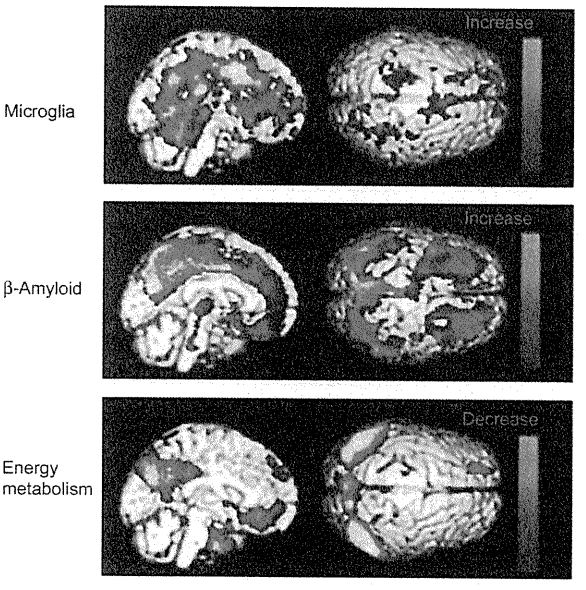

Figure 4 Regions with statistically significant increases in microglial activation and β-amyloid, and significant decrease in energy metabolism.
Modified from Yokokura et al. (2010).